Application of different spatial sampling patterns for sparse array transducer design. ☆☆

Svetoslav Ivanov Nikolov and Jørgen Arendt Jensen

Center for Fast Ultrasound Imaging, Department of Information Technology,
Build 344, Technical University of Denmark, 2800 Lyngby.

Abstract

In the last years the efforts of many researchers have been focused on developing 3D real-time scanners.

The use of 2D phased-array transducers makes it possible to steer the ultrasonic beam in all directions in the scanned volume. An unacceptably large amount of transducer channels (more than 4000) must be used, if the conventional phased array transducers are extrapolated to the two-dimensional case. To decrease the number of channels, sparse arrays with different aperture apodization functions in transmit and receive have to be designed.

The design usually is carried out in 1D, and then transfered to a 2D rectangular grid. In this paper 5 different 2D array transducers have been considered and their performance was compared with respect to spatial and contrast resolution. An optimization of the element placement along the diagonals is suggested. The simulation results of the ultrasound fields show a decrease of the grating-lobe level of 10 dB for the diagonally optimized 2D array transducers.

BibTex Entry:

```
@article{ref_nikolov_jensen_2000,
  title     = "Application of different spatial sampling patterns
               for sparse-array transducer design",
  publisher = "Elsevier BV",
  author    = "Svetoslav Nikolov and Jensen, {Jørgen Arendt}",
  year      = "2000",
  doi       = "10.1016/S0041-624X(00)00013-5",
  volume    = "37",
  number    = "10",
  pages     = "667--671",
  journal   = "Ultrasonics",
  issn      = "0041-624X",
```

Keywords: Two-dimensional, Sparse, Array, Transducer(s)

1. Introduction

To obtain a three-dimensional scan of the body, an ultrasound scanner must be able to focus in any direction of the interrogated volume. This can be obtained either by mechanically rocking a focused transducer or by electronically steering the ultrasound beam as shown in Fig. 1. The latter makes it possible also to implement parallel receive beamforming and to do the scanning in real time [1]. The system is considered to be linear, and can thus be characterized by its point-spread-function (PSF). Ideally the PSF is a spatial δ function. Side-lobes are present in the radiation pattern due to the finite size of the transducers . The periodic nature of the linear arrays introduces grating lobes. The grating lobes are outside the scanned region if the spacing between the elements is $\lambda/2$. To obtain high resolution with a small number of channels, arrays with a pitch of $p > \lambda/2$ must be used and the grating lobes enter the viewed field.

Randomly sparsed arrays do not have a periodical sampling pattern and thus they do not have prominent grating lobes in the radiation pattern. However, a pedestal of side-lobe energy at level of approximately -30 dB from the peak value is present. Although some optimization can be applied on the weighting coefficients [2], the performance can not be increased to a level comparable to the dense arrays.

The ultrasound system must be evaluated in terms of the two-way (transmit and receive) radiation pattern. A formal approach is introduced by the use of the *coarray* [3] also known as *effective aperture* [4].

☆Paper presented at Ultrasonics International'99 World Congress on Ultrasonics'99, 29 June – 1 July, 1999, Lyngby, Denmark.

*Corresponding author,
E-mail address: nikolov.svetoslav on gmail (S.I. Nikolov)
**E-mail address: jaj at elektro dtu dk

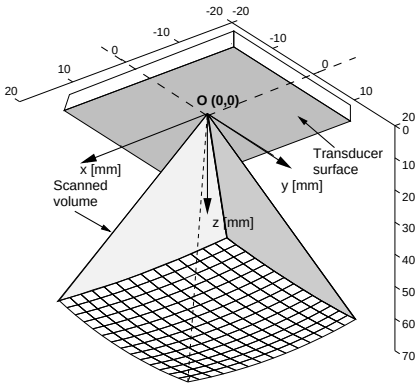

Figure 1: Volumetric scanning. The center of the coordinate system is in the middle of the transducer surface.

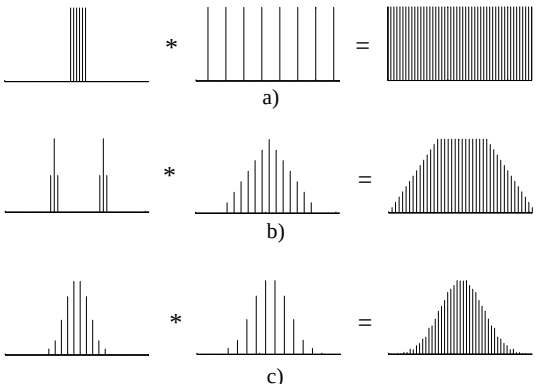

Figure 2: Transmit, receive and effective apertures. The resulting effective aperture, from top to bottom, has rectangular, triangular and cosine^2 apodizations

The effective aperture is briefly introduced in Section 2 and Section 3 shows how it can be used to design linear transmit and receive apertures. In Section 4 the design is extended to 2D. Section 5 gives the radiation patterns of these apertures obtained by computer simulations of ultrasound fields.

2. Effective aperture concept

The effective aperture of an array is the aperture that has a radiation pattern identical to the two-way (transmit and receive) radiation pattern of the array. The connection between the array aperture function $a(x/\lambda)$ and the radiation pattern in the far field and in the focal region $P(s)$ is given by the Fourier transform [1]:

$$P(s) = \int_{-\infty}^{+\infty} a\left(\frac{x}{\lambda}\right) e^{j2\pi(x/\lambda)} d\left(\frac{x}{\lambda}\right) \quad (1)$$

where the aperture function describes the element weighting as a function of the element position, $s = \sin\phi$, ϕ is the angle measured from the perpendicular to the array, and x/λ is the element location in wavelengths. The two way radiation pattern is

$$P_{TR}(s) = P_T(s)P_R(s) \quad (2)$$

The radiation pattern of the effective aperture can be expressed as a spatial convolution of the transmit and receive apertures.

$$E(x/\lambda) = a_T(x/\lambda) * a_R(x/\lambda) \quad (3)$$

The design of the transmit and receive apertures is thus reduced to the problem of finding a suitable effective aperture with a desired Fourier transform. The elements in the effective aperture must be spaced at $\lambda/2$, and the weighting function shouldn't have discontinuities to avoid the side and grating-lobes. Since the radiation pattern is the Fourier transform of effective aperture, it is convenient to exploit the properties of the classical windowing functions : rectangular, triangular and hamming. These functions are separable, and the design can be carried out in 1D and then extended to 2D.

3. Aperture design strategies in 1D

Fig. 2 shows three different design strategies leading to an effective aperture with $\lambda/2$ spaced elements.

A simple approach, shown in Fig. 2 a) is to select a dense transmit aperture with N_{xmt} elements. Its width is $D_{xmt} = N_{xmt}\lambda/2$. The receive aperture must then have spacing between its elements $d_{rcv} = (N_{xmt} - 1)\lambda/2$. Hereby a fully populated effective aperture is obtained with the minimum number of elements in the transmit and receive apertures. Because of the rectangular shape of the apodization function, of the effective aperture, this design will be further referred to as "rectangular approximation".

Fig. 2 b) shows how an apodized effective aperture can be obtained by introducing some redundancy in the number of transmit and receive elements. From the properties of the Fourier transform it is expected that this design has lower sidelobes than the design depicted in Fig. 2 a). Further in the paper this kind of effective aperture will be referred to as "triangular", and the design as "triangular approximation".

The transmit aperture has two active sub-apertures. The spacing between two active elements is $\lambda/2$. The number of active elements is $2N_{act}$. The width of the active sub-aperture is $D_{act} = N_{act}\lambda/2$. The spacing between the elements in the receive aperture is $d_{rcv} = D_{act}/2$. If it has N_{rcv} active elements, its size is $D_{rcv} = (N_{rcv} - 1)D_{act}/2$. The spacing between the two active sub-apertures is $d_{sub} = D_{rcv}/2$.

Fig. 2 c) shows how to obtain effective aperture, apodized with the coefficients of a Hamming window. In [4] these arrays are called “vernier arrays” and therefore this term will be used further in the article. The spacing of the arrays is chosen to be $n\lambda/2$ and $(n-1)\lambda/2$, where n is an integer number. This guarantees that the spacing between the samples of the effective aperture is $\lambda/2$. Additional apodization gives control over the radiation pattern. For the apertures in Fig. 2 a value of $n = 3$ was used. From the properties of the hamming window it can be expected that this configuration would yield the lowest side and grating lobes, at the expense of decreased resolution.

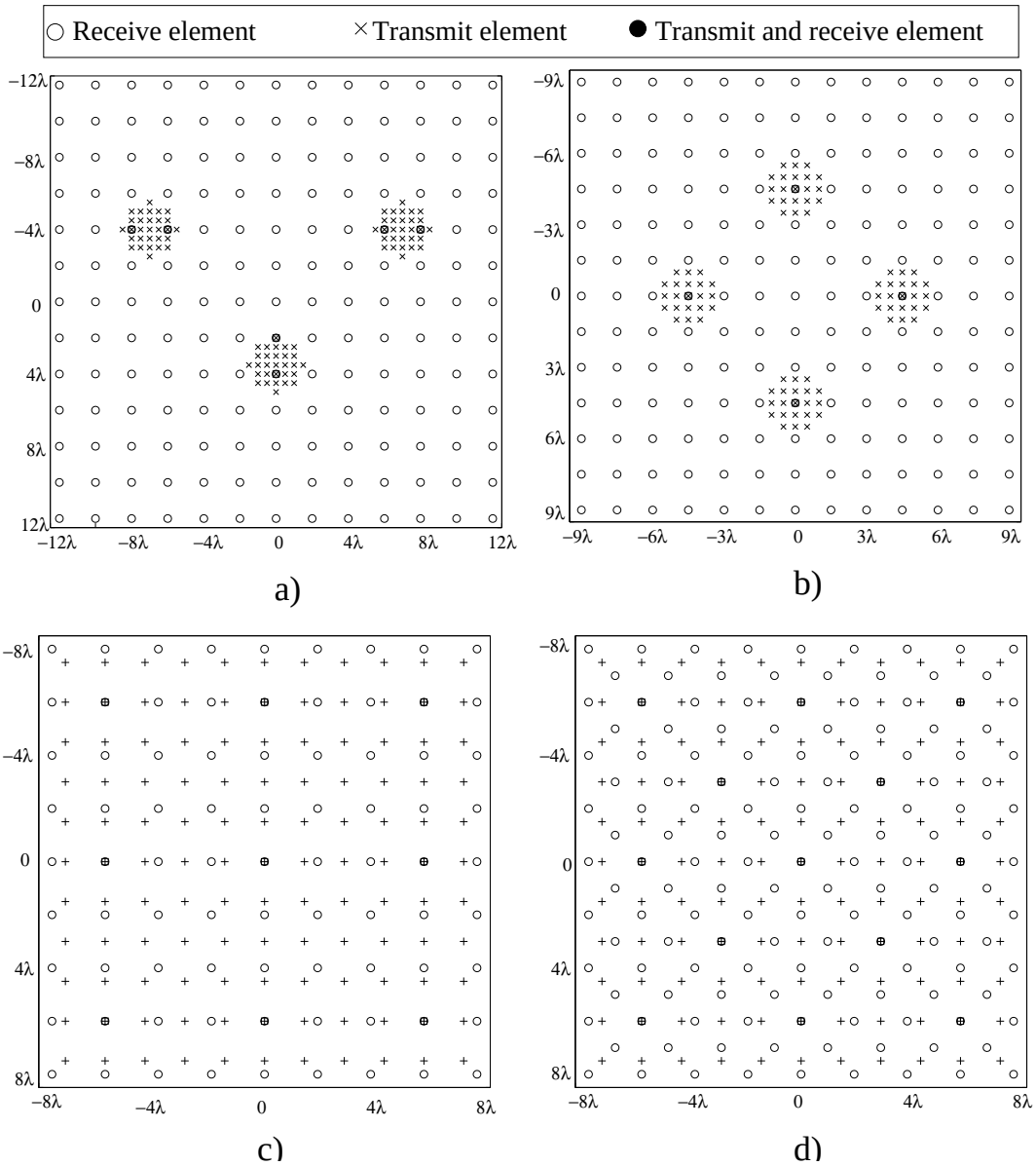

Figure 3: The transmit and receive aperture geometries. From bottom down: apertures for triangular approximation; vernier arrays with triangular sampling pattern.

4. Transition to 2D

After the apertures are created in the one-dimensional case, their design must be extended to the two-dimensional space. Usually a rectangular grid is used for sampling of the transducer surface. The distance between two elements along the same row or column is $\lambda/2$.

The extension of the rectangular approximation to 2D is straight forward. Let the transmit aperture be a rectangular grid of size 11x11 elements, spaced at $\lambda/2$ distance. The horizontal and vertical spacing between the elements of the receive grid, in this case is 5λ.

Fig. 3 a) and b) show two examples of triangular approximations. The resulting effective aperture is shown in Fig. 4. Configuration a) has more transmit elements in a single active sub-aperture than configuration b). To maintain the same number of elements aperture a) has less active sub-apertures.

The vernier approximation can also be extended to the two-dimensional case by selecting the element spacing independently for the x and y axes, as it was previously done in [4]. Such configuration is shown in Fig.3 c) and will be further referred to as "rectangular vernier approximation". The spacing between the elements in the receive aperture is $4\lambda/2$ and in the transmit aperture it is $3\lambda/2$. The vernier nature of the sampling grid is preserved along the rows and the columns but is broken along the diagonals. This results in high grating lobes in the $(x-z)$ and $(y-z)$ planes. In Fig. 4 d) a new, diagonally optimized pattern is suggested. A new element is inserted in the diagonal direction between every two receive elements. In this way the element spacing along the diagonals in the receive aperture becomes $2\lambda/\sqrt{2}$. The diagonal spacing in the transmit aperture is $\lambda/2$, thus keeping the vernier nature of the sampling pattern

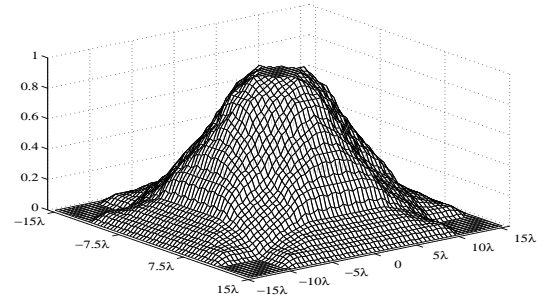

Figure 4: Effective aperture obtained by a triangular approximation.

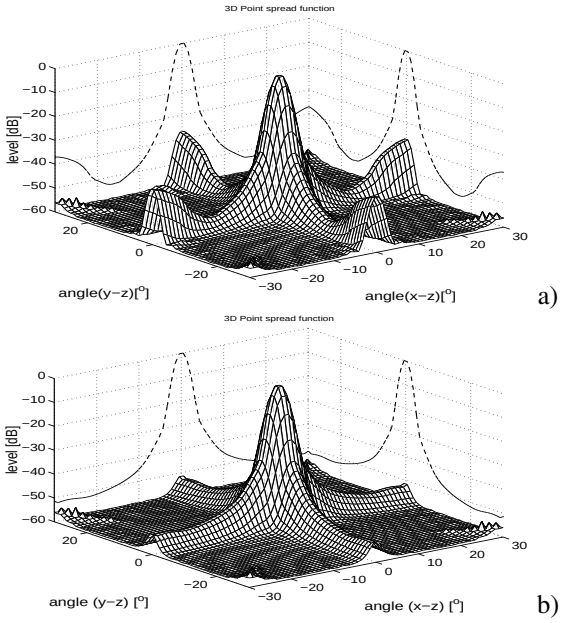

Figure 5: Point spread functions. The arrays are designed using: a) Vernier interpolation b) Diagonally optimized Vernier approximation.

along the diagonals. According to the Fourier transform, this design decreases the grating-lobe energy with more than 5 dB.

5. Simulation results

All simulations are made by the program Field II [5]. A 60°x60° volume containing a single point scatterer is scanned. The point-spread function is obtained by taking the maximum in a given direction. The simulation parameters are listed in Table 1.

Parameter	Notation	Value	Unit
Speed of sound	c	1540	m/s
Central Frequency	f_0	3	MHz
Sampling Frequency	f_s	105	MHz
Pitch	p	0.5	mm
Bandwidth	BW	70	%

Table 1: Simulation parameters.

Design Method	-3dB deg.	-6dB deg.	MSR dB	Peak dB
Rectangular	1.21	1.67	30.6	-32.1
3 Clusters	2.15	2.81	47.7	-41.3
4 Clusters	3.09	4.04	49.8	-42.2
Rect Vernier	2.37	3.09	51.3	-38.0
Trian Vernier	2.61	3.57	51.8	-49.1

Table 2: Simulation results. The table shows the -3dB and -6dB beam-widths, the mainlobe-to-sidelobe energy ratio (MSR), and the highest level of the grating lobes.

The size of the transmit and receive apertures are dependent on the design method. The apertures were designed to contain a total of 256 transmit and receive channels. Fig. 5 shows two point-spread functions: a) a Vernier approximation, extended to 2D on a rectangular grid [4], and b) a Vernier approximation optimized along the diagonals. The diagonal optimization results in almost 10 dB decrease of the highest grating lobe level. From Table 2 it can be seen that the loss of resolution at -3 dB is 9%.

The point spread function $PSF(\theta,\phi)$ is a function of the azimuth and elevation angles θ and ϕ. The main lobe can be defined as:

$$ML(\theta,\phi) = \begin{cases} 1, & 20\lg(\frac{PSF(\theta,\phi)}{PSF(0,0)}) > -30 \\ 0, & otherwise \end{cases}$$

The mainlobe-to-sidelobe energy ratio is calculated by :

$$MSR = \frac{\sum\sum |PSF(\theta,\phi)|^2 \, ML(\theta,\phi)}{\sum\sum |PSF(\theta,\phi)|^2 \, (1 - ML(\theta,\phi))}$$

The contrast of the image is dependent on this ratio. Table. 1 shows that the aperture obtained by the rectangular approximation has the highest resolution. Unfortunately it forms a side-lobe pedestal at -33 dB and performs poorly in viewing low-contrast objects like cysts. On the other hand, the apertures formed using triangular approximation have lower resolution, but the level of side-lobe and grating-lobe energy decreases with the angle. Thus distant high-radiation regions do not influence the dark regions in the image and images with higher contrast can be obtained. The diagonally optimized vernier array has the highest MSR and has the potential of yielding images with the highest contrast at the expense of a 9% reduced resolution.

6. Conclusion

The periodic arrays have lower side-lobe energy than the sparse arrays and they have the potential of giving images with higher contrast. The *effective aperture concept* is a fast and

easy way to design sparse arrays with desired properties. The design can be first implemented in 1D and then extended to 2D. The results from simulations on Vernier arrays show that radiation patterns with higher MSR are obtained when the design includes the diagonals of the rectangular grid.

7. Acknowledgements

This work was supported by grant 9700883 and 9700563 from the Danish Science Foundation, and by a grant from B-K Medical A/S.

[1] S. W. Smith, H. G. Pavy, and O. T. von Ramm. High-speed ultrasound volumetric imaging system – Part I: Transducer design and beam steering. *IEEE Trans. Ultrason., Ferroelec., Freq. Contr.*, 38:100–108, 1991.

[2] Bjørnar Elgetun Sverre Holm and Geir Dahl. Properties of the beampattern of weight-and-layout-optimized arrays. *IEEE Trans. Ultrason., Ferroelec., Freq. Contr.*, 44:983–991, 1997.

[3] Ralph T. Hoctor and Saleem A. Kassam. The unifying role of the coarray in aperture synthesis for coherent and incoherent imaging. *IEEE Proc.*, 78, 1990.

[4] G. R. Lockwood and F.S. Foster. Optimizing sparse two-dimensional transducer arrays using and effective aperture approach. In *Proc. IEEE Ultrason. Symp.*, pages 1497–1501, 1994.

[5] J. A. Jensen. Field: A program for simulating ultrasound systems. *Med. Biol. Eng. Comp.*, 10th Nordic-Baltic Conference on Biomedical Imaging, Vol. 4, Supplement 1, Part 1:351–353, 1996b.